Geom. Ded. Vol. 23, No. 3 (1987)

BARRY MONSON

A FAMILY OF UNIFORM POLYTOPES WITH SYMMETRIC SHADOWS

ABSTRACT. A peculiar manipulation of the Coxeter diagrams used in Wythoff's construction provides a family of orthogonal projections of one uniform polytope onto another.

1. INTRODUCTION

In [5] Coxeter exhibited an orthogonal projection of the vertices of the E_8 polytope 4_{21} onto those of a pair of concentric 600-cells whose circumradii are in the golden ratio $\tau:1$ (where $\tau = (1 + \sqrt{5})/2$). This example is just one of a large and interesting class of orthogonal projections from $2n$-space to n-space, here derived by manipulating Coxeter diagrams in a way 'compatible' with Wythoff's construction. We note that Peter McMullen has independently encountered many of our examples as part of unpublished work on realizations of regular polytopes; we also thank him and the referee for suggesting several improvements.

We first choose a basis $\{e_1, \ldots, e_{2n}\}$ for $\mathbb{R}^{2n}$ and write $x \in \mathbb{R}^{2n}$ uniquely as

$$x = (u, v) = \sum_{j=1}^{n} u_j e_j + v_j e_{j+n}$$

for row vectors $u, v \in \mathbb{R}^n$. Now fix a non-zero real λ and define a linear map $\varphi: \mathbb{R}^{2n} \to \mathbb{R}^{2n}$ by

(1.1) $$\varphi(x) = \varphi(u, v) = (1 + \lambda^2)^{-1}(u + \lambda v, \lambda u + \lambda^2 v).$$

Next equip $\mathbb{R}^{2n}$ with a symmetric bilinear form '·' whose Gram matrix

$$M = \begin{bmatrix} A & B \\ B & C \end{bmatrix}$$

has symmetric $n \times n$ blocks A and B, while

(1.2) $$C = A + (\lambda - \lambda^{-1})B.$$

In the orthogonal geometry $(\mathbb{R}^{2n}, \cdot)$ we routinely check:

(1.3) (a) The map φ is an orthogonal projection onto the n-dimensional subspace $S = \{(w, \lambda w): w \in \mathbb{R}^n\}$.

(b) For all $x = (u, v)$, $x' = (u', v')$

$$\varphi(x) \cdot \varphi(x') = (1 + \lambda^2)^{-1}[u + \lambda v][A + \lambda B][u' + \lambda v']^t.$$

This work was supported by the NSERC of Canada (Grant A4818).

(c) For $1 \leqslant i \leqslant n$, let $d_i = (1+\lambda^2)^{1/2}\varphi(e_i)$. Then $\varphi(e_{i+n}) = \lambda\varphi(e_i)$ and the basis $\{d_1, \ldots, d_n\}$ for S has a Gram matrix $\hat{M} = A + \lambda B$.

(d) By replacing λ by $\eta = -\lambda^{-1}$, we replace φ by its complement $\psi = \mathrm{Id} - \varphi$, whose image space is $T = \{(-\lambda v, v): v \in \mathbb{R}^n\}$. Thus $T \subseteq S^\perp$, with equality if and only if $\hat{M}$ is invertible.

In what follows $M = [-\cos(\pi/p_{ij})]$ is the Coxeter matrix for the Coxeter group G with presentation

$$\langle r_1, \ldots r_{2n} | (r_i r_j)^{p_{ij}} = 1, 1 \leqslant i, j \leqslant 2n\rangle,$$

where all $p_{ii} = 1$, and for $i \neq j$, $p_{ij} \in \{2, 3, 4, \ldots, \infty\}$; (delete any relation with $p_{ij} = \infty$). G is represented faithfully in GL($2n$, $\mathbb{R}$) [1, p. 91], where, for $1 \leqslant i \leqslant 2n$, we take r_i to be the reflection

$$r_i: x \to x - 2(x \cdot e_i)e_i \quad (x \in \mathbb{R}^{2n}).$$

Both M and G are conveniently represented by a Coxeter diagram Δ on $2n$ nodes; when $p_{ij} \neq 2$, nodes i and j are joined by a branch labelled p_{ij}, though the frequent label '3' is omitted and understood. The most interesting examples, when G is finite and irreducible and M has signature $(+ + \cdots +)$, are indicated in Figure 1(a)–(d). Nodes $1, \ldots, n$ appear across the top row, with nodes $n+1, \ldots, 2n$ just below. The symmetry of B forces symmetrical connections between the rows, so that these examples, in which G acts on spherical space S^{2n-1}, are easily selected from the list in [2, p. 297]. Similarly, if M has signature $(+ + \cdots + -)$, as in Figure 3(a), (b), we may take G as acting on hyperbolic space H^{2n-1}. In both cases, a fundamental region for G is

$$L = \{x \in \mathbb{R}^{2n}: x \cdot e_i \geqslant 0, 1 \leqslant i \leqslant 2n\}$$

which (considering point coordinates as homogeneous up to positive multiples) describes a simplex bounded by the mirrors for the r_i, with dihedral angles π/p_{ij} and vertices v^j, where $e_i \cdot v^j = \delta_i^j$, $1 \leqslant i, j \leqslant 2n$.

In the only degenerate cases considered here, M has signature $(+ + \cdots + 0)$ with null space spanned by $m = (m_j) = (1, 1, \sqrt{2}, \sqrt{2})$ for Figure 2(a) and $m = (1, 1, \ldots, 1)$ for Figure 2(b), (c), etc. To model the action of G on Euclidean space E^{2n-1} we must use the dual space $L(\mathbb{R}^{2n})$ (of linear functions) with basis $\{f^1, \ldots, f^{2n}\}$ satisfying $f^j(e_i) = \delta_i^j$. Then as described in [1, pp. 92–99], G acts in the contradredient way on

(1.4) $$E^{2n-1} = \{f \in L(\mathbb{R}^{2n}): f(m) = 1\}$$

with fundamental simplex

$$L = \{f \in E^{2n-1}: f(e_i) \geqslant 0, 1 \leqslant i \leqslant 2n\}$$

having vertices $v^j = m_j^{-1} f^j$.

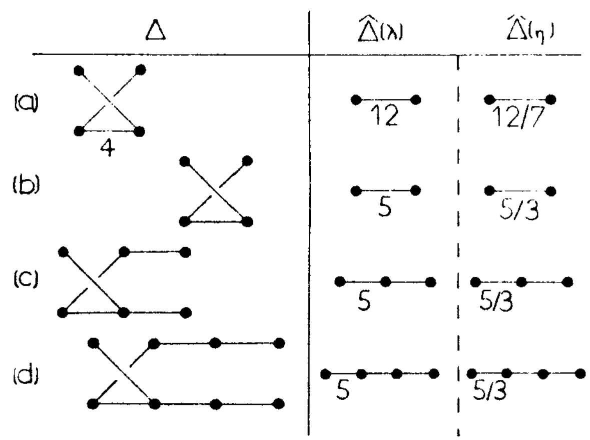

Fig. 1. Spherical diagrams.

2. A SUBGROUP GENERATED BY HALF-TURNS

Let H be the subgroup of G generated by the half-turns $h_i = r_{i+n} r_i$, $1 \leqslant i \leqslant n$. We henceforth

(2.1) Assume that the diagram Δ has no nodes i and $i+n$ adjacent. (Thus B has vanishing diagonal and we avoid graphs such as that in Figure 3(c).)

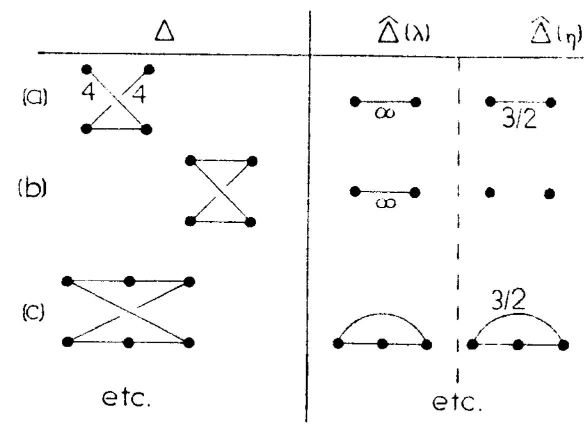

Fig. 2. Euclidean diagrams.

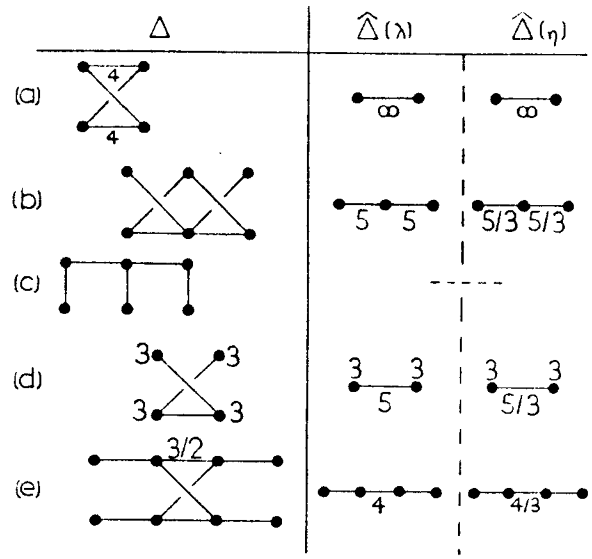

Fig. 3. Other Coxeter diagrams.

We easily check that this assumption is equivalent to:

(2.2) For $1 \leqslant i \leqslant n$, φ and ψ each commute with h_i.

By (1.3(c)) each $d_i \cdot d_i = 1$, so that the new reflections

$$\hat{r}_i: x \to x - 2(x \cdot d_i)d_i, \quad x \in S,$$

generate a group $\hat{G}$ of isometries acting on S. In fact:

(2.3) Each h_i fixes S (and T) and equals $\hat{r}_i$ on S.

Furthermore, a case by case check yields

(2.4) PROPOSITION. *The group $\hat{G}$ is a Coxeter group with matrix $\hat{M} = A + \lambda B$ and diagram $\hat{\Delta}(\lambda)$, displayed next to Δ in the figures.*

Proof. From (1.2), $a_{12} + (\lambda - \lambda^{-1})b_{12} = c_{12}$. For each Δ compute $\hat{M}$ then $\hat{\Delta}(\lambda)$, noting that $\hat{r}_i\hat{r}_j$ has period q_{ij} if $\cos(\pi/q_{ij}) = -d_i \cdot d_j = -[a_{ij} + \lambda b_{ij}]$. For instance, in Figure 1(a), $0 + (\lambda - \lambda^{-1})(-\frac{1}{2}) = -1/\sqrt{2}$, so that $\lambda = (1 + \sqrt{3})/\sqrt{2}$ and $q_{12} = 12$, and $\eta = -\lambda^{-1} = (1 - \sqrt{3})/\sqrt{2}$ with $t_{12} = \frac{12}{7}$. □

(2.5) REMARK. Each result is displayed in the figures, which also include the diagrams $\hat{\Delta}(\eta)$ which arise when λ is replaced by η. Even with a non-integral branch label q_{ij}, $\hat{\Delta}(\eta)$ still describes a simplex L with dihedral angle π/q_{ij}, if not immediately the corresponding group. □

Now the period of h_ih_j is determined by its action on the complementary spaces S and T. Noting, for instance, that a rotation through $2\pi(5/3)$ has period 5 we verify:

(2.6) PROPOSITION. *For each group G with diagram Δ in Figures 1(a)–3(b), the subgroup H generated by the half-turns $h_1, \ldots, h_n$ is isomorphic to the group $\hat{G}$ with diagram $\hat{\Delta}(\lambda)$ (pair h_i with $\hat{r}_i$).*

(2.7) EXAMPLE (Figure 1(d)). The E_8 group $G = [3^{4,2,1}]$ has $H \simeq \hat{G} = [3, 3, 5]$ as a subgroup generated by half-turns. Clearly, in both G and $\hat{G}$ the product of the generators must have 'Petrie' period $h = 30$ [2, pp. 221, 234].

3. Wythoff's construction and examples

In Wythoff's construction [2, p. 196] we ring certain nodes of Δ thereby describing a uniform polytope (or honeycomb) Π whose vertex set Π_0 is the G-orbit of a point $v \in L$, which is equidistant from mirrors corresponding to ringed nodes but lies on the remaining mirrors. Likewise, a standard p-face F of Π is specified by the subgraph Δ_p of Δ induced on those nodes corresponding to mirrors fixing F (setwise); of course, the G-orbit of F provides other faces of Π congruent to F. In fact, since Δ_p is the Coxeter graph for the stabilizer G_p of F in G, there are $[G: G_p]$ faces of Π equivalent to F. Note that Δ_0 is the subgraph on unringed nodes [2, p. 197].

Suppose the ringed nodes are $j, \ldots, k + n, \ldots$ for certain $j, k \in \{1, \ldots, n\}$. Then, for some $\alpha > 0$ and all $i \in \{1, \ldots, n\}$

(3.1) (a) $v = \alpha[v^j + \cdots + v^{k+n} + \cdots]$

(b) $d_i \cdot \varphi(v) = \alpha(1 + \lambda^2)^{-1/2}[(\delta_i^j + \cdots) + \lambda(\delta_i^k \cdots)]$.

Since $\hat{G} \simeq H \subseteq G$, we also find that

(3.2) $\varphi(\Pi_0)$ contains the $\hat{G}$-orbit of $\varphi(v)$ and is the union of the vertex sets of various $\hat{G}$-symmetric (perhaps non-uniform) polytopes in S.

Furthermore, if each r_i is rational with respect to the basis $\{e_1, \ldots, e_n\}$, and λ is irrational, then $\varphi(w) \neq \varphi(z)$ for distinct $w, z \in \Pi_0$. Hence, for those polytopes derived from Figures 1(b)–(d), 3(b), distinct p-faces of Π project to distinct (though perhaps overlapping) convex subsets of $\varphi(\Pi)$. Compare Example (3.6) below, with $\lambda = 1$.

(3.3) EXAMPLE. The regular 4-simplex α_4 is defined by ringing node 1 of Δ in Figure 1(b). By 2.6, $\hat{G} \simeq D_5$, the symmetry group of the regular pentagon {5}. Hence, the 5 vertices and 10 edges of α_4 project onto those of a {5}, together with its vertex figures, which form an inscribed pentagram

5/3}. Other faces of α_4 such as the {3} specified by Δ_2 on nodes 1 and 4, are reshortened by φ[2, p. 120]. □

Trivially, all vertices and edges of Π have uniform projections. For the tandard p-face F, $\varphi(F)$ (and its $\hat{G}$-images in S) will be uniform only when he ringed nodes in Δ_p are properly disposed. If $\varphi(F)$ is uniform, then each on-zero $d_i \cdot \varphi(v)$ must take one value, so that (3.1(b)) forces one of several onditions on the ringed nodes in Δ: no bottom nodes, no top nodes, $\lambda = 1$ nd no nodes j and $j + n$ both ringed, etc. For brevity we consider just one ase abundant with examples.

3.4) PROPOSITION. *Suppose the standard p-face F of* Π *has a graph* Δ_p *hose ringed components have all nodes* $j, k, \ldots \in J \subseteq \{1, \ldots, n\}$ *(thus* $p \leqslant n$*). lso suppose that in* Δ *no node* $k + n$ *is ringed or is adjacent to node j, for any* $k \in J$. *Then* $\varphi(F)$ *(or any* $\hat{G}$*-image) is a uniform p-face of the polytope* $\hat{\Pi}$ *efined in S by ringing nodes j, k, … of* $\hat{\Delta}(\lambda)$ *for* $j, k \in J$. *Each such face of* $\hat{\Pi}$ *rises by projection of a* Π*-face equivalent to F, and they are enumerated by nalyzing the ringed graph* $\hat{\Delta}(\lambda)$.

Remarks. Notice that $\hat{\Pi} \subseteq \varphi(\Pi)$. As in Example (3.3) Π generally has eftover faces equivalent under G to F, which have other uniform or non-niform projections. Some sort of condition on the nodes of *both* Δ and Δ_p s needed to force $\varphi(F)$ to be uniform.

Proof. Let $j, k \ldots \in J$. The given assumptions, with (2.1) and (2.3), imply hat

$$\begin{aligned}\varphi[(r_j r_k \ldots)v] &= \varphi[(h_j h_k \ldots)v] \\ &= (h_j h_k \ldots)\varphi(v) = (\hat{r}_j \hat{r}_k \ldots)\varphi(v).\end{aligned}$$ □

The analysis of specific cases depends on the combinatorial pecularities of he groups G and $\hat{G}$. We therefore conclude with a variety of examples ased on (3.4), whose details are readily verified by hand or machine. nvariably, $\hat{\Delta} = \hat{\Delta}(\lambda)$ from the figures.

.5. *Other Uniform Polytopes*

a) Ring node 3 from Δ and $\hat{\Delta}$ in Figure 1(c). Using (3.3) to analyze the ertex figures, we find that the 12 vertices, 60 edges and 40 of the 160 riangular faces of the cross polytope β_6 project onto corresponding lements of the icosahedron {3, 5}, with an inscribed great icosahedron {3, /3}; cf. [2, p. 254]. Ringing node 1 instead provides a projection from a set f alternate vertices of the 6-cube onto those of a dodecahedron and eciprocal icosahedron.

(b) Ringing node 4 from Δ in Figure 1(d) we obtain the E_8 polytope 4_{21}, whose 240 vertices give unit normals for the mirrors of reflection in the E_8 group. Using 3.5(a) for the vertex figures, we find that the vertices and certain edges, triangles and tetrahedral faces from 4_{21} project onto those of a concentric {3, 3, 5} and {3, 3, 5/3} with circumradii in the ratio τ:1: cf [5].

(c) Ringing node 1 in Figure 1(a) provides a projection of the vertices and certain edges of the 24-cell {3, 4, 3} onto those of a concentric {12} and {12/7} (in contrast with (a), (b) the inner dodecagon is rotated $\pi/12$ with respect to the outer; cf. [2, pp. 149, 245–247]).

(d) By ringing nodes 1 and 2 from Δ in Figure 1(b) we obtain the α_4 polytope $t_{0,3}\alpha_4$, whose 20 vertices are the unit normals to the hyperplanes of symmetry of α_4. The projection φ yields concentric polygons {10} and {10/3} with circumradii in the ratio τ:1. (The remaining 40 edges of α_4 connect the two decagons.) The conditions of (3.4) are not satisfied here: indeed $\varphi(\Pi)$ is more symmetrical than first expected.

(e) In the complex reflection groups described in Figure 3 (d), each r_i has period 3. Nevertheless, our results apply since we can take M real, with entry $-1/\sqrt{3}$ for adjacent nodes in Δ [3, p. 132]. As in Figure 1(b), $(\lambda, \eta) = (\tau, -\tau^{-1})$. Ringing node 1 of Δ provides an orthogonal projection of the 240 vertices, and a certain 240 edges, of the Witting polytope 3{3}3{3}3{3}3 onto the vertices and edges of concentric polygons 3{5}3 and 3{5/3}3, with circumradii in the ratio τ:1 (cf. [6, pp. 192–193] for a dual result, and [3, pp. 105, 134] for the connection with (b) above).

(f) A diagram Δ with a fractional label still describes a simplex. In Figure 3(e) we consider just one of many available examples: here $(\lambda, \eta) = (1 + \sqrt{2}, 1 - \sqrt{2})$. Now let

$$\begin{aligned}e'_4 &= -e_1, \\ e'_3 &= -(01111221) = r_4 r_3 r_6 r_7 r_5 r_8 r_6 r_7(-e_2),\end{aligned}$$

and

$$e'_1, e'_2, e'_5, e'_6, e'_7 \text{ resp. } e'_8 = e_5, e_4, e_3, e_6, e_7, \text{ resp. } e_8.$$

Then $M' = (e'_i \cdot e'_j)$ is the Coxeter matrix for the E_8 diagram in Figure 1(d). In fact, in the present example G is the E_8 group (generated in a 'starry' way). By ringing node 4 of Δ we obtain a starry uniform polytope Π with the same vertices, edges and triangular faces as the polytope 4_{21} described in 3.5(b). The 240 vertices project in sets of 24 + 24, 144 and 24 + 24 to three concentric hyperspheres with radii in the ratio $\lambda^{1/2}:2^{1/4}:\lambda^{-1/2}$. The inner and outer sets each belong to a pair of reciprocal {3, 4, 3}'s, while the ices of the middle set belong to the truncation defined by ringing nodes ıd 4 in the diagram $\hat{\Delta}(\lambda)$ in Figure 3(e).

;) *Remarks*. The complementary projection ψ provides a similar set of ılts. If several nodes of Δ are ringed, we cannot expect the projected ices to yield just one or two uniform polytopes since $[G{:}H]$ is generally e.

Euclidean Honeycombs

:e the graph Δ in Figure 2(a) describes the symmetry group of the ıliar cubic lattice in E^3, we consider only the infinite family of groups , $n \geqslant 2$, given in Figures 2(b), (c), etc. Since $\lambda = 1$ and φ fixes the null or m, the adjoint φ^* acts naturally on E^{2n-1} (see (1.4)). The image of orthogonal projection is the Euclidean space E^{n-1} through the points of edges $(v^1, v^{1+n}), \ldots, (v^n, v^{2n})$ of L. By ringing node 1 in Δ, and ı, we describe honeycombs $\alpha_{2n-1}h$ in E^{2n-1} and $\alpha_{n-1}h$ in E^{n-1} [4, pp. 152]; in fact, φ^* maps the vertices of the former onto those of the latter, ı covered infinitely often. The complementary projection ψ^* (with -1) has non-canonical image space since $\psi(m) = 0$; and for $n \geqslant 3$, the esponding diagram $\hat{\Delta}(\eta)$ is an n-gon with one branch labelled '3/2'. ections in the walls of the resulting simplex generate the D_n group with ısity' 2^{n-2} [4, pp. 161–164]. Thus the vertices of $\alpha_{2n-1}h$ project onto ıe of infinitely many concentric polytopes with D_n symmetry. Here we $D_3 = A_3$, $D_2 = A_1 \times A_1$.

Hyperbolic Honeycombs

Let Π be the honeycomb in H^3 defined by ringing node 1 of Δ in Figure Now φ is the orthogonal projection onto the line S perpendicular to :s (v^1, v^3) and (v^2, v^4) of the fundamental simplex L. The planes through e edges and perpendicular to S enclose a fundamental region of infinite me for H. Since L is compact, it easily follows that the vertices of Π ect onto a dense subset of S.

ı) Such non-discrete behaviour attends the example in Figure 3(b). By ıparing the action of the subgroup H on S and on $T = S^{\perp}$, we observe the group [5, 5] acting discretely on the hyperbolic plane is isomorphic ıe non-discrete group generated by reflections in the sides of a spherical ıgle K with angles $3\pi/5$, $3\pi/5$ and $\pi/2$; thus K is not a Schwarz triangle). 20].

REFERENCES

1. Bourbaki, N., *Groupes et Algèbres de Lie*, Chaps. iv–vi, Hermann, Paris, 1968.
2. Coxeter, H. S. M., *Regular Polytopes*, Dover, New York, 1973.
3. Coxeter, H. S. M., *Regular Complex Polytopes*, Cambridge Univ. Press, New York, 1974.
4. Coxeter, H. S. M., 'The Derivation of Schönberg's Star Polytopes from Schoute's Simplex Nets', *The Geometric Vein – the Coxeter Festschrift*, Springer, New York, Berlin, 1981, pp. 149–164.
5. Coxeter, H. S. M., 'The 600-Cell {3, 3, 5} as a Shadow of 4_{21}, the E_8 Polytope', *Math Forchungs. Oberwolfach, Tagungsber.* **31** (1981).
6. Coxeter, H. S. M., 'Surprising Relationships among Unitary Reflection Groups', *Proc. Edinburgh Math. Soc.* **27** (1984), pp. 185–194.

Author's address:

Barry Monson,
Department of Mathematics,
University of New Brunswick,
Fredericton, N.B. E3B 5A3,
Canada

(Received, August 7, 1985; revised version, May 28, 1986)